

# COMBINED DYNAMIC MECHANICAL ANALYSIS (DMA) AND CALORIMETRY FOR CURE MONITORING OF COLD-CURED THERMOSET AND ITS HOLLOW PARTICLE REINFORCED COMPOSITE

M. Salvia<sup>1</sup>, M. Bouslah<sup>1</sup>, I. Deschères<sup>2</sup> and H. Baurier<sup>3</sup>

<sup>1</sup>Laboratoire de Tribologie et de Dynamique des Systèmes, Ecole Centrale de Lyon, 36 avenue Guy de Collongue, 69134, Ecully, France, Email: [michelle.salvia@ec-lyon.fr](mailto:michelle.salvia@ec-lyon.fr), web page: <http://ltds.ec-lyon.fr>

<sup>2</sup>Génie de la Fonctionnalisation des Matériaux Polymères, Institut Textile et Chimique de Lyon, 87 chemin des mouilles, 69134 Ecully, France, Email: [isabelle.descheres@itech.fr](mailto:isabelle.descheres@itech.fr), web page: <http://www.itech.fr>

<sup>3</sup>METRAVIB, ACOEM group, 200 chemin des Ormeaux, 69578 Limonest, France, Email: [hugues.baurier@acoemgroup.com](mailto:hugues.baurier@acoemgroup.com), web page: <http://METRAVIB.acoemgroup.fr/dma>

**Keywords:** DMA, Thermal flux, Shrinkage, Curing, Thermoset,  $\alpha$ -Relaxation, CTE, DIC

## ABSTRACT

This study proposes to monitor the cure of a phenolic system for impregnation by hand into glass fibers and its composite reinforced with glass microballoons at room temperature using a thermal flux cell combined with a DMA. The HFC200 cell, developed by METRAVIB allows the simultaneous monitoring of thermal (sample temperature and thermal flux), mechanical (complex stiffness) and dimensional changes on the same sample in the same experimental conditions. This point is particularly important because the thermoset reaction is exothermic, so kinetic parameters depend strongly on the sample geometry and quantity. Particular attention will be given to the changing of physical properties, from the liquid to the solid state by investigating the effects of different factors (catalyst rate, volume) on cure kinetic behaviour of the phenolic matrix and its composite (filler volume fraction: 0.45). The influence of the mixture composition on final properties of materials will be then analysed in terms of position of the  $\alpha$ -relaxation peak, and volume changes.

## 1 INTRODUCTION

Phenolic resin based composites are increasingly used in high-tech areas due to their superior fire and flammability properties by comparison with other composite based thermosetting resins such as polyester or epoxy. Indeed, under severe fire conditions phenolic resins have intrinsic resistance to ignition and release minimal quantities of smoke or toxic fumes because of their unique chemical structure which mainly comprises C-C bonds in aromatic rings. These composites find uses in weight sensitive domains mainly in transports (interior) and marine applications. In this last field, the main applications are mostly lightweight sandwich structures for fire resistance and insulation which combine hand lay-up made skins and lightweight cores such as syntactic foams well-known for their good thermal insulation properties, low thermal expansion and high specific mechanical properties. For such use phenolic resins have to be tailored for room-temperature cure.

The properties of the resulting mechanical composites are directly in relation to reinforcement type but also to viscoelastic matrix properties and reinforcement/matrix interactions. The most important factor which can control the properties of the matrix and of the reinforcement-matrix interface is in particular the cross-linking density resulting from the manufacturing process that is linked to the degree of cure. The cure of a thermoset is a complex process which leads to a three-dimensional macromolecular network. The final morphology of the three-dimensional network, which determines

the properties of the material, depends on this transformation. During the thermoset resin cure, there is an interaction between chemical kinetics and physical changes, which may involve an incomplete degree of conversion of the system. Two phenomena may appear during the reaction according to the cure temperature: gelation and/or vitrification [1]. Gelation is the liquid to rubber transition, which occurs when the system reaches a certain degree of conversion corresponding to the time when an infinite network is formed. This transition is not frequency dependent. Vitrification is rubber to glass transition, which occurs when the glass transition increases to the temperature of cure. This transition is frequency dependent. For an optimization of the manufacture of thermosetting based composite parts, a better understanding of mutual influence of thermal and mechanical history on the material process and final properties will therefore be of great use.

This study proposes to monitor the cure of a phenolic system and its composite reinforced with glass microballoons (filler volume fraction: 0.45) at room temperature using a thermal flux cell combined with a DMA. The influence of curing conditions on final properties of materials will be then analysed in terms of position of the  $\alpha$ -relaxation peak and volume change measurements versus temperature.

## 2 MATERIALS

Phenolic prepolymers are obtained by condensation reaction of phenol with formaldehyde. The strong base-catalysed reaction containing an excess of formaldehyde leads to resole phenolic prepolymers. The prepolymer used in this study is a low-molecular-weight resin (370 g/mole) available as an aqueous solution (Dynea). The system is neutralized (pH = 7.5) and has a viscosity of 221 mPas and a solid content of 72 % by weight (NF EN ISO 325 standard) and its glass transition temperature,  $T_{g0}$  is  $-64^{\circ}\text{C}$  (taken at midpoint with 10 K/min heating rate). This mixture is stored at a temperature between  $5\text{-}10^{\circ}\text{C}$  before cross-linking process. This cross-linking process involves a condensation reaction as for synthesizing the prepolymer which requires temperature and/or catalysts (acid or basic). In this work, the curing was carried out at room temperature using a mixture of two acid catalysts: *p*-toluene sulfonic acid (PTSA) and partial phosphate ester which is also a flame retardant additive. The reinforcements for core are glass hollow microspheres from 3M Company having diameters in the range 15-85 micrometres and a density of  $0.38\text{ g/cm}^3$ . Their pH (9.4) was measured using NF EN ISO 787-9 standard [2]. Different unfilled and filled mixtures (catalyst weight fraction) and volumes were tested as given in Table 1.

Mixture	Reference	PTSA (wt.%)	Phosphate ester (wt.%)	Filler volume fraction	Volume mL
RES-1	RES-1-50	0.75	0.5	–	50
RES-2	RES-2-50	1.5	1	–	50
	RES-4-5	3	2	–	5
RES-4	RES-4-25	3	2	–	25
	RES-4-50	3	2	–	50
RES-8	RES-8-50	6	4	–	50
SF-8	SF-8-50	6	4	0.45	50
SF-16	SF-16-50	12	8	0.45	50

Table 1: Tested mixtures

## 3 EXPERIMENTAL METHODS

In this paper, the curing of the phenolic resin and its composite at room temperature was investigated using a classical dynamic mechanical analysis (DMA) device equipped with a specific cell with flux sensors. After curing the sample were analysed using DMA, CTE measurements and bending tests up to failure.

### 3.1 Dynamic mechanical analysis and thermal flux cell for cure monitoring

Dynamical mechanical analysis (DMA) provides convenient and sensitive determination of thermo-mechanical properties of polymers and reinforced polymers at solid or liquid state as a function of frequency and temperature. It consists in either applying a sinusoidal force to a material and measuring the displacement or applying a displacement and measuring the displacement. The displacement is lagged behind the force by a phase angle  $\delta$  due to the viscoelastic characteristics of the polymers [3]. From the force and displacement measurements the complex stiffness can be deduced,  $K^* = K' + jK''$  where  $K'$  is the storage stiffness and  $K''$  is the loss stiffness. The loss factor is the ratio of loss stiffness to storage stiffness  $\tan \delta = K''/K'$ . Knowing the sample geometry either complex tensile ( $E^*$ ) or shear modulus ( $G^*$ ) can be obtained depending on the deformation mode. This method is particularly appropriate to analyse the relaxation processes ((main) and sub- $T_g$ ) of polymer-based materials [4]. DMA can also provide valuable information for monitoring curing progression of thermoset as the material changes from viscous liquid state to infusible cross-linked solid (3D-network). This transformation may involve two main transitions: gelation when the viscous liquid prepolymer is transformed in an infusible, insoluble gel or rubber-like material and vitrification which corresponds to rubber-glass transition. At vitrification the rate of the cure reaction may be significantly reduced due to molecular mobility. This phenomenon occurs only if the reactive mixture is cured at a temperature lower than the infinite glass transition temperature of completely cross-linked system. This occurs when the glass transition temperature ( $T_g$ ) equals the cure temperature.

The point at which gelation occurs can be detected following different criteria, depending on author and kind of tests or materials. The gelation occurs at a given conversion point at which mass average molecular weight becomes infinite. Consequently, gelation onset is independent of timescale of observation (frequency-independent) and at this instant the elastic component of the system exceeds the viscous component. When the measure concerns reactive liquid mixture (neat resin) the gelation point can be estimated from the intersection of the storage modulus and the loss modulus as a function of time curves at a given frequency, loss modulus being orders of magnitude larger than storage modulus at liquid state, i.e. when the loss factor  $\tan \delta$  is equal to 1. It is not generalized for all thermoset systems and devices. For certain of them, if this crossover exists, it might be frequency-dependent [5]. The instant of gelation also can be detected when the loss factor  $\tan \delta$  momentarily becomes frequency independent. If the two previous methods are not applicable the gel time may be also determined as the intersection between the tangent line at storage modulus versus time curve and the baseline or the inflexion point of this curve. After gelation the network becomes denser through further cross-linking reaction. A direct result is the glass transition temperature ( $T_g$ ) of the system increase as the mobility of polymer chain decreases. When the cure temperature is equal to the  $T_g$  of the thermoset the vitrification occurs. When using dynamic mechanical method vitrification is commonly determined as the frequency dependent peak of  $\tan \delta$ . The frequency dependence of  $\tan \delta$  obeys the following relationship:  $\omega\tau = 1$  where  $\tau$  is the relaxation time and  $\omega$  the frequency and therefore more the test frequency is elevated more the  $\tan \delta$  peak is shifted to shorter time.

In this study resin cure monitoring were carried out on a Metravib DMA+ 450 viscoanalyser. This set-up consists of an axial electro dynamic shaker, in the upper part of the frame and a piezoelectric force transducer in the lower part of the frame. This DMA was equipped with a specific tool for cure monitoring (HFC200) mounted in between the excitator and the force sensor. This tool provides in the same experiment information on mechanical changes, chemical and/or thermal shrinkage and thermal phenomena according to time during polymerization of thermoset resin [6]. It consists of two plates with a cylindrical closed cavity of 5 mL between them in which the liquid reactive resin sample is injected (Figure 1a). This tool is fitted with heat flux sensors located on upper and lower plates. For volume greater than 5 mL (up to 50 mL), the cylindrical cavity was removed and replaced by a transparent container. In this case the measurement of the thermal flux was only performed by the upper sensor. After filling the sample container, the upper plate was brought in close contact with the liquid sample and the set-up adjusts the position of the upper plate during test so that it is always in continuous contact with the sample even if shrinkage or expansion may occur. Thickness or volume (isotropic material) changes and complex stiffness were obtained using static displacement and dynamic force

measurements respectively. As the oven was not used the curing process was also followed using the change of color and opacity as a function of time (Figure 1b).



Figure 1 Metravib DMA+ 450 viscoanalyser equipped with thermal flux tool: (a) cell for  $V= 5\text{mL}$  and (b) Cell for volume up to 50 mL.

After curing the materials were machined into a rectangular parallelepiped with dimensions of about  $28 \times 5 \times 4 \text{ mm}^3$  and DMA tests were performed in tension-compression mode.

### 3.2 Coefficient of thermal expansion ((CTE) measurements using Digital Image Correlation (DIC)

Coefficient of thermal expansion (CTE) testing was carried out on machined cured samples using a climate chamber equipped with a window on top developed by France Etuves and Digital image stereo correlation (DISC) (Figure 2a). This technique is an optic contactless experimental technique to measure displacements and deformations and is well suited for CTE measurements [7]. The image capturing system consists of two CCD cameras (AVT Pike F-421B) with the resolution  $2048 \times 2048$  pixels providing monochromatic images with 14 bit of dynamic range. The software used in this study converts the 14 bit images to 8 bit (256 grey levels). The cameras field of view is  $250 \times 250 \text{ mm}$ . (1 pixel on the CCD sensor corresponds to a  $0.12 \text{ mm}$  square on the specimen). To illuminate the sample and to limit reflections, the white lights are inside the climate chamber. Two thermocouples are fixed on the rear side of the specimen and in the climate chamber respectively. The specimen is painted with aerosol black and white spray paint to create a speckle pattern with adequate contrast (Figure 2b) To measure strain due to free thermal expansion, pairs of images are taken at room temperature defining the reference state of the object. Then the temperature is increased progressively. Images are taken, every  $25^\circ\text{C}$  from  $30^\circ\text{C}$  to  $300^\circ\text{C}$ , when the specimen temperature is stabilized. A square region of interest (ROI) was selected in the middle of the specimen. This zone delimits the area over which the displacements are measured. A view of a resole phenolic resin with the subset grid numerically superimposed on the disc is shown in Figure 2c. The subset size was  $31 \times 31$  pixels and the step was 7. The DISC software VIC 3D was used to compute the Lagrange strain tensor.

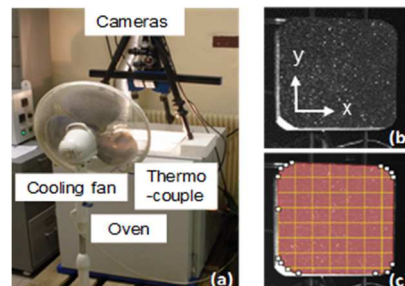


Figure 2: (a) View of the experimental set up for CTE measurements; (b) Cured Resole resin sample. (c) ROI and subsets ( $31 \times 31$  pixels)

## 4 RESULTS AND DISCUSSION

### 4.1 Cure monitoring

Figure 3a shows complex stiffness  $K^*$ ,  $\tan \delta$  measured by coupled calorimetry-DMA analysis at 5, 10 and 20 Hz during cure at room temperature for RES-4-50 mixture. Figure 3b presents the static displacement and thermal results (heat flux and temperature) vs time for the same specimen. At the very early beginning, the complex stiffness was quasi-practically constant ( $K' \sim 10$  N/m) during about  $\sim 20$  min. During this time the results were quite noisy and difficult to measure for frequencies above 5 Hz. Beyond this lag-time the storage stiffness  $K'$ , showed a two-step increase with a first plateau occurring near 32 min after a large increase in  $K'$  by more than three decades ( $K' \sim 10^6$  N/m). The second plateau ( $K' \sim 1,8 \cdot 10^7$  N/m) was reached after about 36 min. After the lag-time, the loss stiffness exhibited versus time a large increase until the storage stiffness  $K'$  equals the loss stiffness  $K''$  ( $K' = K''$  or  $\tan \delta = 1$ ). At this moment  $K''$  slightly decreased, increased again and then went to a maximum ( $t_{\max} = 35.9$  min for 20 Hz and  $t_{\max} = 37.4$  min for 5 Hz), before decreasing and reaching a plateau ( $\sim 10^5$  N/m). At about 30 min the loss factor  $\tan \delta$  became independent of the test frequency (crossover of the curves of  $\tan \delta$  versus time) and then showed a dependent frequency peak occurring at shorter times with increasing frequency as for  $K''$ . The maximum of  $\tan \delta$  occurred at the midpoint of the storage stiffness variation versus time.

At the very beginning, the thermoset mixture was composed of low-molecular prepolymers resulting then in a low stiffness. As the reaction proceeded, chain extension occurred to produce relatively high molecular weight reaction products resulting in an increase of stiffness. Gelation which corresponds to the first appearance of an infinite cross-linked network was associated in this study to the time at which the loss factor vs time curves measured at different frequencies intersected. Indeed, the intersection of the curves of  $K'$  and  $K''$  according to time was frequency-dependent. The gel time was confirmed by the analysis of static displacement vs time. The point at which  $\tan \delta$  became frequency independent (i.e. crossover of the loss angles) corresponded to the instant at which the material began to develop a significant modulus and a significant change in static displacement was observed. The static displacement which was representative of thickness or volume (isotropic material) variation changed little during a period of about 30 min after which it increased slightly and then tended to decrease sharply. Then, the drop in static displacement rate appeared to slow down after about 40 min. As the resin was in a liquid state it may flow at the edge of the cell (configuration 2). Gelation marks the moment at which the material can support a load without flowing due to the occurrence of elastic behavior and then led to static displacement evolution. The heat of reaction resulted in a rise in temperature from room temperature up to about 56 °C at 37 min after which it decreased slowly (Figure 3b). The volume changes were therefore driven by two competing mechanisms: thermal expansion and volumetric shrinkage. During heating up the thermal expansion took over in the very early stages of the gelation process, and then the shrinkage associated to chemical cross-linkings dominated. Beyond the temperature maximum the volumetric shrinkage of the resole resin was a combination of chemical and thermal shrinking. The slight slowdown of the drop of the static displacement may be associated to vitrification zone as it was observed in the time domain of the occurrence of the second  $\tan \delta$  peak, which was frequency-dependent. As mentioned previously, vitrification is associated with the transition from a rubbery modulus to a glassy modulus. At this condition, the mobility of the reacting groups was hindered and restricted with the reduction of free volume. Thereby, this phenomenon led to an extremely slow reaction, with the reaction rate now controlled by diffusion rather than being controlled by chemical factors.

The results for the other mixtures using the same analysis are summarized in Table 2. From this Table, it was observed that, for a given sample volume (50 mL), the cure of unfilled resin was accelerated by increasing the amount of catalysts (RES-x-50 with x (proton rate) = 1, 2, 4, 8). The greater catalyst proportion, the lesser the gel time and vitrification time and the higher the heat of reaction and the reaction rate. The rate of cure of resole resin was also dependent of the volume of the blend, all other things remaining equal (RES-4-5, RES-4-25, RES-4-50).

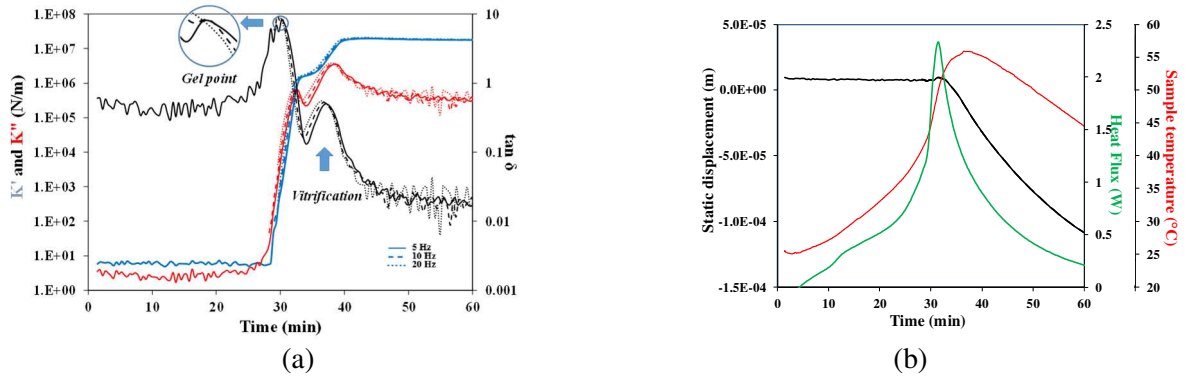


Figure 3: (a)  $K'$ ,  $K''$  and  $\tan \delta$  (b) static displacement, mixture sample temperature and heat flux vs time for RES-4-25

Table 2 shows there was a critical volume below which there was not enough heat which was liberated within 120 min because of the very low reaction rate. Curing the resin under ambient temperature was helped by heat of reaction which introduces a temperature rise of the mixture which depends on the volume of the resin and the heat transfer boundary.

Compound	Volume mL	Gel time $t_{gel}$ (min)	Vitrification time $t_{vit}$ at 10 Hz (min)	Exothermal peak		Heat flux peak	
				Temperature (°C)	Time (min)	Heat flux (W)	Time (min)
RES-4-5	5	>>120	>>120	/	/	0.00	/
RES-4-25	25	36.0	49.3	44.5	36.9	0.7	32.8
RES-4-50	50	30.4	37.1	55.9	36.9	2.4	31.4
RES-1-50	50	>> 600	>> 600	29.4	75.0	0.06	57
RES-2-50	50	610	>> 610	33.2	50.0	0.2	35.2
RES-8-50	50	9	10.0	62.3	15.5	4.6	8.7
SF-8-50	50	>> 20 h	>> 20 h	/	/	/	/
SF-16-50	50	4.8	10.8	48.9	8.4	3.6	3.1

Table 2: Tested compounds and curing results

The optical analysis performed on resin mixture named RES-4-25 (Figure 4) confirmed thermomechanical analyses.

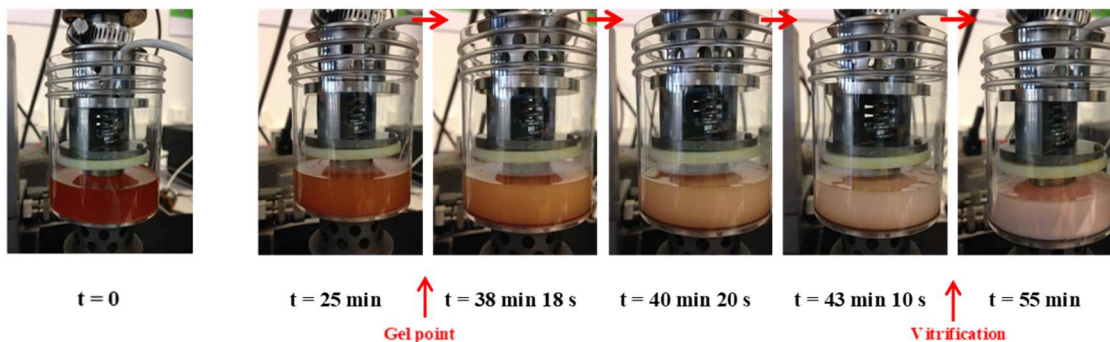


Figure 4: Optical analysis of RES-4-25 mixture cure as a function of time

The clear initial mixture became after the gel point more and more cloudy due to the occurrence of an increasing fraction of insoluble and moisture condensation (water as by-product) which causes micropores to develop in the blend as shown Figure 5 [8]. As the cross-linking reaction occurred at ambient temperature or slightly above ( $T$  at exothermal peak is about  $45^\circ\text{C}$ ), the voids were filled with water.

After vitrification, a completely opaque material was obtained. Its color evolved gradually towards the pink because of the oxidation of residual traces of phenol and by-products not having reacted.

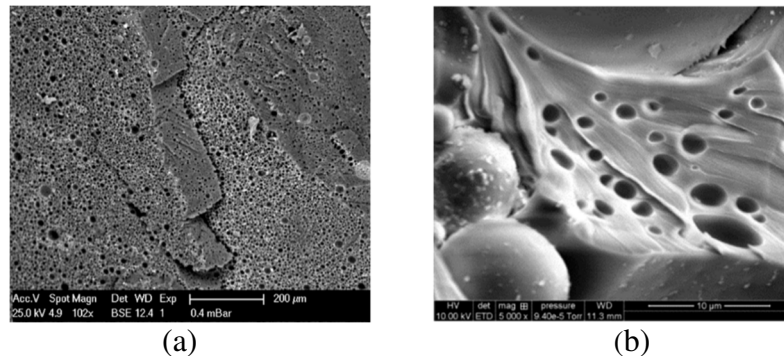


Figure 5: SEM micrographs of failure feature of unfilled (a) and filled with glass micro-balloons (b) resole thermoset showing the porous structure of the resin

As can be seen in Table 2, the use of glass micro balloons has an inhibiting effect. For the same catalyst content curing reactions of filled resole were much slower than for neat matrix and the values of the gel times reached several hours. The inhibition effects of glass microspheres may be due by different causes: steric hindrance caused by the sorption of the reacting monomers on the surface of fillers (physisorption), basic pH of fillers which slows down the role of catalysts, reduced volume of resin involved in the mixture. They can also interfere with functional groups of the reacting monomers (hydrogen-bonds).

## 4.2 Characterisation of cured specimen

### *Evaluation by DMA*

It is well known that main relaxation measurements associated to  $T_g$  can be used as an accurate indication of cross-link density of a thermosetting. The thermomechanical properties were analyzed using DMA on both neat and filled with glass microspheres resin after curing and stabilization at room conditions (23°C, 50% HR) during one month.

Tests were carried out studied in tension-compression mode at controlled dynamic displacement ( $\pm 5 \mu\text{m}$ ) in the linear viscoelasticity domain. Two successive temperature sweeps were carried out at a heating rate of 1 K/min in 0 - 250 °C temperature range. The measuring frequency was from 0.1 Hz to 10 Hz. Typical plots of the storage modulus  $E'$  and the loss factor  $\tan \delta$  versus temperature for RES-2-50 compound during 1<sup>st</sup> run were given in Figure 6a. The results were not presented above 200°C, because an important shrinkage due to bound water removing.  $E'$  decreased slightly up to about 60°C (0.1 Hz) from which a frequency-dependant change in slope was observed. The lower the frequency the earlier the slope appeared. This phenomenon was related to the onset of the main relaxation  $T_\alpha$  associated to the glass transition. Unlike what was usual, the height of the step in storage modulus was different from one frequency to another and the peak in loss factor was not frequency-dependent and quite broad ( $\Delta T = 100^\circ\text{C}$ ). For the lowest frequency (0.1 Hz) a slight increase in storage modulus was observed just after the rubbery plateau was reached. The evolutions of  $E'$  and  $\tan \delta$  vs temperature resulted from the competition between two factors: the occurrence of the actual  $\alpha$ -relaxation of the material at the initial state (devitrification) leading to an increase of mobility of macromolecule segments and in the free volume which allowed the ongoing curing reaction and progress in cross-linking reactions within temperature increase. The volatility of the solvent (bound water molecules around 100 °C) may also be responsible for the broadening of the peak. These analyses pointed out that after curing and stabilization one month at room temperature a full degree of curing was not achieved.



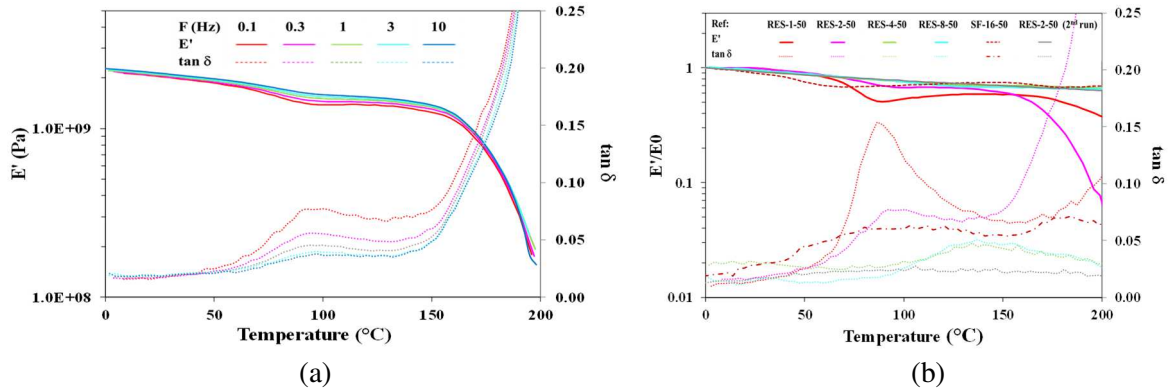


Figure 6: Temperature dependences of  $E'$  and  $\tan \delta$  response for cured (a) compound (RES-2-50) as a function of frequency (b) compounds ((RES-x-50) and (SF-16-50) ( $F=0.1$  Hz)

Results were roughly the same for the other formulations. Figure 6b shows the influence of catalyst level (compounds: RES-x-50 with x, number of protons 1, 2,4,8) and fillers (SF-16-50) on the thermomechanical behaviour after curing. The more the catalyst rate was high, the more: the drop of the storage modulus and the amplitude of the loss factor peak associated to the primary relaxation of the resin were low. The onset of the modulus drop and the maximum of  $\tan \delta$  were shifted towards high temperatures and the area under the curve of loss factor was reduced. These features were consistent with a progressive decrease in chain motion due to a degree of crosslink increase with catalyst level. The cure inhibition effect caused by filler led to a reduced cross-linking density (occurrence of  $E'$  drop at the lowest T).

The improvements in mechanical stability at high temperatures caused by post-curing and volatilization of plasticizer as water was illustrated in Figure 6b which gave the results ( $E'$  and  $\tan \delta$  vs T) after a previous run until  $200^{\circ}C$  (RES-2-50: 2<sup>nd</sup> run). The post-curing and drying were evident from these results: the material showed a more classical behaviour with a flat single frequency-dependant peak of  $\tan \delta$ . Nevertheless, the broadness of this peak indicated that the polymerized network was heterogeneous.

### Comparison with DIC volume change measurements

Typical plots of the mean values of the strains ( $\epsilon_{xx}$  and  $\epsilon_{yy}$ ) obtained for the two specimens (RES-2-50) and (SF-16-50) according to temperature were given in Figure 7 (a) and (b) respectively. These variations were compared to the results from DMA (0.1 Hz) for the same specimens.

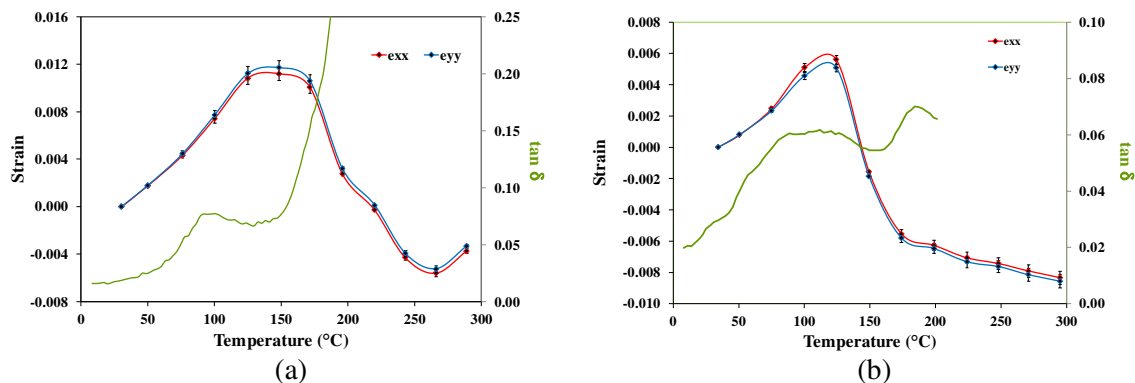


Figure 7: Strain evolutions as a function of temperature and  $\tan \delta$  vs T (0.1 Hz) for (a) un filled and (b) filled resin

In-plane strains were quasi-similar in the two directions (x) and (y) confirming the isotropic nature of the materials. When the temperature raised, the strain exhibited a linear dependence with temperature below the onset of the main relaxation (around  $60^{\circ}C$ ). The unfilled resin exhibited an average CTE value



of  $1,16 \times 10^{-4}$  K. The CTE value of the filled resin is about 40 % lower than the CTE of the neat resin due to low CTE of the glass beads (mixture law). As the temperature increases above 60°C, the strain changes vs temperature were driven by different competing mechanisms as discussed previously: glass transition, thermal expansion, shrinkage due to residual reaction and water removing.

## 5 CONCLUSIONS

In this study, the effect of acid catalyst rate and volume of blend was investigated on the curing and the properties of the formed network of an ambient-cured resole resin and its composite filled with hollow glass microspheres for civil engineering applications. Gelation and vitrification, but also thermal properties (sample temperature, heat flux) which knowledge is very important for the design of resin formulation were determined using a DMA (METRAVIB DMA+450) equipped with a specific tool (HFC200) allowing the simultaneous monitoring of viscoelastic, calorimetric and changes in volume information. These results showed that multidetection monitoring provided a powerful tool for understanding the changes in physical properties of resole thermoset during cure. The viscoelastic analysis of cured sample after staying one month at room temperature showed that the materials were not fully cured but that the evolution occurred above the use temperature conditions (ambient temperature). This was confirmed by strain changes according to temperature measured by DIC method.

## REFERENCES

- [1] J. P. Pascault, H. Sautereau, J. Verdu and R. J. J. Williams, *Thermosetting Polymers*, Marcel Dekker, New York, 2002.
- [2] AFNOR, NF EN ISO 787-9, Détermination du pH d'une suspension aqueuse, *Méthodes générales d'essai des pigments et matières de charge*, 1995.
- [3] J. D. Ferry, *Viscoelastic Properties of Polymers*, 3<sup>rd</sup> Ed, Wiley, New York, 1980.
- [4] B. Kechaou, M. Salvia B. Beaugiraud, D. Juvé, Z. Fakhfakh and D. Treheux, Mechanical and dielectric characterization of hemp fibre reinforced polypropylene (HFRPP) by dry impregnation process, *eXPRESS Polymer Letters*, **4**, 2010, pp. 171-182 (doi: [10.3144/expresspolymlett.2010.22](https://doi.org/10.3144/expresspolymlett.2010.22)).
- [5] H.H. Winter, Can the gel point of a cross-linking polymer be detected by the  $G' - G''$  crossover?, *Polymer Engineering & Science*, **27**, 1987, pp. 1698-1702 (doi: [10.1002/pen.760272209](https://doi.org/10.1002/pen.760272209)).
- [6] C. Billotte, F. M. Bernard and E. Ruiz, Chemical shrinkage and thermomechanical characterization of an epoxy resin during cure by a novel in situ measurement method, *European Polymer Journal*, **49**, 2013, pp. 3548-3560 (doi: [10.1016/j.eurpolymj.2013.07.013](https://doi.org/10.1016/j.eurpolymj.2013.07.013)).
- [7] C. Flament, M. Salvia, B. Berthel and G. Crosland, Digital Image Correlation applied to Thermal Expansion of Composites, *Proceedings of the 19th International Conference on Composite Materials (ICCM-19) 2013 (eds S Van Hoa and P Hubert), 28 July–2 August, 2013, Montreal, Canada, 2013*, pp. 5235–5243.
- [8] S. Feih, Z. Mathys, G. Mathys, A.G. Gibson and A.P. Mouritz, Influence of water content on failure of phenolic composites in fire, *Polymer Degradation and Stability*. **93**, 2008, pp. 376-382 (doi.org/10.1016/j.polyimdegradstab.2007.11.027).